

M. Szala^{1,*}, M. Walczak^{1,2}, L. Łatka³, K. Gancarczyk⁴, D. Özkan⁵

¹Lublin University of Technology, Department of Materials Engineering, Lublin, Poland

²University of Economics and Innovation, Faculty of Transport and Computer Science, Lublin, Poland

³Wrocław University of Science and Technology, Faculty of Mechanical Engineering, Wrocław, Poland

⁴Rzeszow University of Technology, Faculty of Mechanical Engineering and Aeronautics, Rzeszow, Poland

⁵National Defense University, Turkish Naval Academy, Mechanical Engineering Department, Tuzla-Istanbul, Turkey

* *m.szala@pollub.pl*

CAVITATION EROSION AND SLIDING WEAR OF MCrAlY AND NiCrMo COATINGS DEPOSITED BY HVOF THERMAL SPRAYING

ABSTRACT

The investigation into wear resistance is an up-to-date problem from the point of view of both scientific and engineering practice. In this study, HVOF coatings such as MCrAlY (CoNiCrAlY and NiCoCrAlY) and NiCrMo were deposited on AISI 310 (X15CrNi25-20) stainless steel substrates. The microstructural properties and surface morphology of the as-sprayed coatings were examined. Cavitation erosion tests were conducted using the vibratory method in accordance with the ASTM G32 standard. Sliding wear was examined with the use of a ball-on-disc tribometer, and friction coefficients were measured. The sliding and cavitation wear mechanisms were identified with the SEM-EDS method. In comparison to the NiCrMo coating, the MCrAlY coatings have lower wear resistance. The cavitation erosion resistance of the as-sprayed M(Co,Ni)CrAlY coatings is almost two times lower than that of the as-sprayed NiCrMoFeCo deposit. Moreover, the sliding wear resistance increases with increasing the nickel content as follows: CoNiCrAlY < NiCoCrAlY < NiCrMoFeCo. The mean friction coefficient of CoNiCrAlY coating equals of 0.873, which almost 50% exceed those reported for coating NiCrMoFeCo of 0.573. The as-sprayed NiCrMoFeCo coating presents superior sliding wear and cavitation erosion resistance to the as-sprayed MCrAlY (CoNiCrAlY and NiCoCrAlY) coatings.

Keywords: *HVOF; thermal spray; coatings; MCrAlY; NiCrMo; cavitation erosion; abrasion; sliding wear*

INTRODUCTION

Cavitation phenomenon is defined as the process of development and growth of vapor bubbles in a fast flowing liquid due to a rapid pressure drop, and then implosions of bubbles at the time of liquid pressure increase. Therefore cavitation causes severe damage to hydraulic machinery [1–3]. Cavitation erosion consists in surface damage and progressive loss of material from a solid due to the action of bubbles in the liquid that systematically collapse at the

surface. It is generally accepted that the impact pressure and shock waves generated by the implosion of cavitation bubbles lead to wear of materials [4–7]. Cavitation erosion is a complex phenomenon, which includes not only hydrodynamic factors of liquid but also properties of erodible material e.g. microstructure, mechanical properties, material surface morphology, etc. [8,9]. Moreover, according to the literature [10–12], the abrasive wear and particularly sliding wear are dominant processes of materials degradation. Furthermore, erosion by solid particles and corrosion is frequently described damage processes in literature [13–17].

Due to the development of new materials and surface treatment techniques, the anti-wear applications are still systematically studied. According to the literature, bulk cobalt- and nickel-based metal alloys have superior resistance to both cavitation erosion and sliding [18–20]. Moreover, Co-, Ni- or even Fe-based overlay deposits are considered highly resistant to both abrasion and erosion [21–23]. It is known that thermally sprayed coatings increase the wear resistance of machine and equipment components and make it possible to prevent or reduce various damage processes. Therefore, different cermet coatings systems have been investigated concerning sliding, abrasive, or erosion wear [24–30]. Despite the fact that the HVOF method allows for metallic or cermet wear-resistant materials deposition [31–33], the anti-wear properties of HVOF coatings are still being investigated. Besides, in comparison to other thermal spraying processes, e.g., plasma spraying or flame spraying, HVOF-deposited coatings exhibit low porosity and crack density, and therefore have a homogeneous structure. This is mainly due to the low thermal stresses, relatively low process temperature, and the high speed of the particles being sprayed [34–36]. It is well known that the homogeneous structure of the material has a positive effect on its resistance to cavitation erosion. Thus, HVOF thermal spraying seems to be the next step in increasing the wear resistance of metallic substrates. Among many thermal spray methods, the HVOF one has some features, which allow producing homogeneous coatings with very low porosity, which is very important in case of abrasive wear, corrosion, and cavitation resistance [37–39]. The primary form of the feedstock material is a powder, but since the last 15 years, many research groups have started to use another type of feedstocks, like suspension and solution ones [40–43]. The detailed description could be found in the work of Pawłowski [44]. Nevertheless, in the field of powder-based HVOF spraying, there is also some modified technique. It is called high-velocity air fuel (HVAF), and the air instead of oxygen is introduced because of the lower cost of the process and results in better properties, especially against wear [45,46].

Currently, new studies on the abrasive wear of thermally deposited coatings are published, and even though these issues seem to be well-known, there are relatively few scientific reports combining both sliding and cavitation testing of HVOF metallic coatings. Mainly, the effect of alloying composition on the cavitation erosion and sliding wear resistance of Ni-Co based matrix coatings deposited by the HVOF method has not been exhaustively investigated.

In this paper, the sliding and cavitation erosion wear resistance of NiCrMoFeCo and MCrAlY (CoNiCrAlY and NiCoCrAlY) coatings was investigated.

EXPERIMENTAL

Materials investigation

The nominal chemical compositions of powders used for the deposition of HVOF coatings are given in Table 1. The substrate was AISI 310 (X15CrNi25-20), with the thickness equal to 8 mm. Coatings thickness was ranging from 180 to 200 μm and the initial roughness

of deposited coatings, *Ra*, was examined with the Dektak 150 contact profilometer (Veeco Instruments, USA). The NiCrMoFeCo and MCrAlY (CoNiCrAlY and NiCoCrAlY) coatings morphology were examined on their top surfaces using a scanning electron microscopy (SEM, Phenom ProX Desktop SEM). The phase composition was estimated by the XRD method, and the procedure is described in [47,48]. The phase composition studies were carried out using a XTRa ARL X-ray diffractometer (Thermo Fisher Scientific, USA). The filtered X-ray radiation of the CuK α 1 lamp $\lambda = 0.154051\text{nm}$ was used applying the Bragg-Brentano diffraction geometry. Parameters that were chosen to obtain the diffractogram: angle range of diffraction pattern $2\theta = 20\text{--}100^\circ$, angular step $2\theta = 0.02^\circ$, counting time for one angular step $t = 6\text{ s}$ and X-ray tube power of 1200W (40 kV and 30 mA). The phase composition was determined using the Powder Diffraction File (PDF) developed and published by ICDD (The International Centre for Diffraction Data) [47,48]. Samples were cutting in order to obtain cross-sections, and it has been prepared by the standard metallographic procedure (impregnate into the resin, then grinding with abrasive papers and polishing with diamond suspension). Hardness was measured on the metallographic cross-sections with a nano-hardness tester (Anton Paar CSM Instruments) having a load of 500 mN accordingly to the reference [36].

Table 1. Nominal chemical composition of feedstock powders

Chemical element, wt.%	Specimen code and coating type		
	A	B	C
	CoNiCrAlY	NiCoCrAlY	NiCrMoFeCo
Ni	32	balance	balance
Co	balance	22	0.5
Cr	21	17	21.5
Al	8	12.5	-
Y	0.5	0.5	-
Mo	-	-	8.5
Fe	-	-	3

Wear examination methods

Sliding wear tests were performed by the ball-on-disc method with a tribotester from CSM Instruments, Switzerland, in compliance with the procedure described in [49]. The idea of the sliding test is presented in Fig. 1. The counter-ball was made of 100Cr6 steel; the applied load was $F=15\text{ N}$, and the sliding distance was set equal to 200 m. The mass loss of the samples was estimated with an accuracy of 0.1 mg. After that, they were examined with the use of a scanning electron microscopy (SEM).

Cavitation erosion tests were conducted using a vibratory rig operating under the conditions given in the ASTM G32 standard [50] and described in the previous paper [51]. The stationary specimen test method and distilled water were used, which is specifically for coatings testing. The gap between horn tip and test surface was set equal to 1 mm, and the amplitude and frequency of the tests were 50 μm and 20 kHz, respectively, while a schematic design of the apparatus is shown in Fig. 2. The specimen is mounted in the holder and submerged in distilled water. Horn tip vibrations generate a cavitation field that causes erosion of the specimen surface (Fig. 2). In the present study, a sonotrode tip with a 15.9 mm diameter was used. The samples were weighed in specified time intervals with an accuracy of 0.01 mg. The worn areas were analyzed with the SEM microscope.

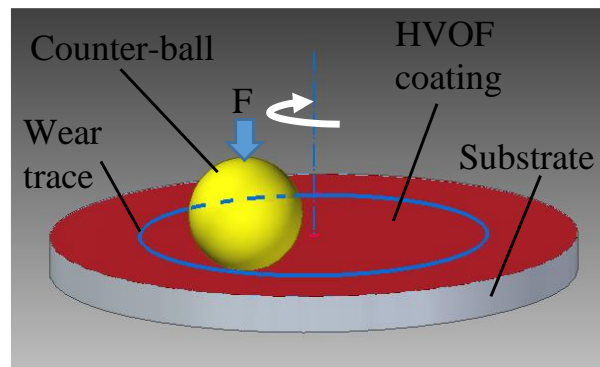


Fig. 1. Scheme of ball-on-disc sliding wear test

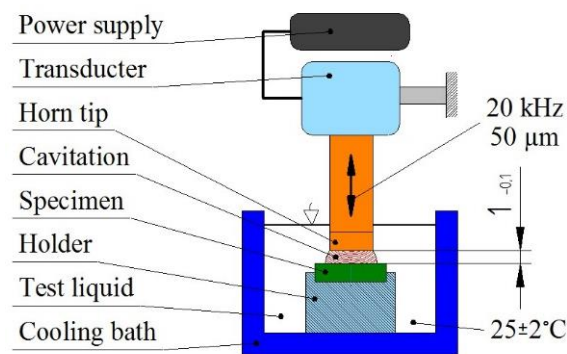


Fig. 2. Design of a vibratory apparatus for cavitation tests

RESULTS

Coating characterization

Results of the surface roughness measurements are given in Table 2. Relative to the relatively low roughness of coatings C, the A coatings exhibit the highest roughness. This observation is confirmed by the SEM examination. The surface morphology of the coatings is presented in Fig. 3-5. The top-view of the coatings indicates their lamellar microstructure and the presence of unmelted powder particles, porosity, and oxides that are typical of thermally sprayed coatings [36,52,53]. According to the XRD analysis results, the coatings A and B form a γ solid solution with the structure of *fcc* and phases β -(Co,Ni)Al and Cr_3Ni , which is in agreement with the data reported in the literature [32,52]. The hardness ranges from 4.8 to 6.0 GPa, which is comparable with the literature data [32,54].

Table 2. The roughness of the as-sprayed coatings

Coating	Roughness, μm				
	Ra	Rq	Rv	Rp	Rt
A	5.94	7.08	-15.27	15.84	31.11
B	5.79	7.20	-16.33	17.73	34.06
C	4.66	5.69	-13.08	13.74	26.83

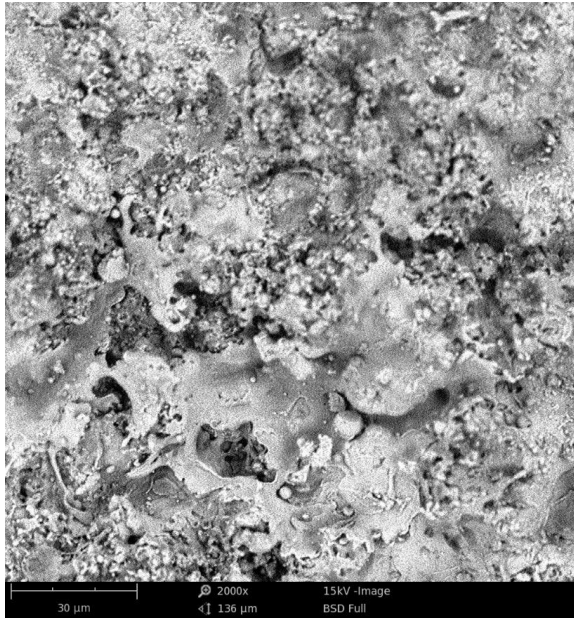


Fig. 3. Surface morphology of coating A (CoNiCrAlY), SEM



Fig. 4. Surface morphology of coating B (NiCoCrAlY), SEM

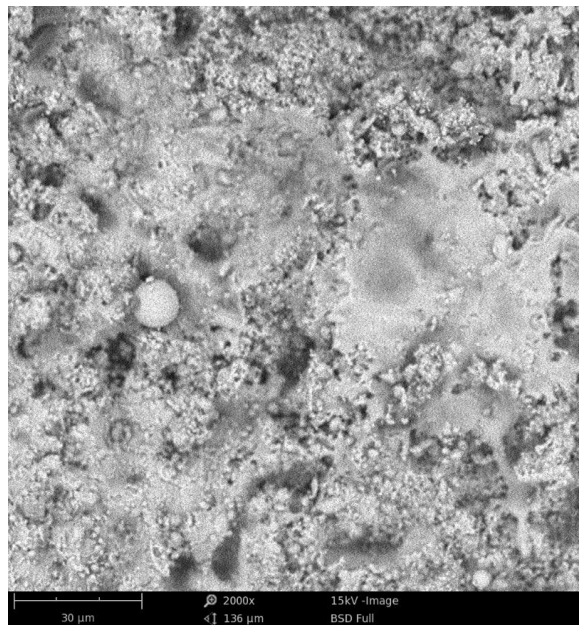


Fig. 5. Surface morphology of coating C (NiCrMoFeCo), SEM

Sliding wear results

Sliding wear results are given in Fig. 6-12 and in Table 3. The results clearly demonstrate that coating A has undergone the highest wear while coating C is the most resistant to wear. The wear resistance of HVOF coatings is lower than reported for nickel, cobalt, and ferrous alloys [20,55]. The friction coefficients are in agreement with the mass loss data, as shown in Fig. 6. At the initial stage of the wear process, the top surface peaks of the coatings are cut out or smashed, and, subsequently, a significant amount of debris occurs in the wear trace. The presence of the wear debris first causes the variation in the coefficient of friction (Fig. 7, Fig. 8 and Fig. 9.), but finally, due to the counter-ball and worn coating fitting, it leads to the sta-

ble coefficient of friction. The wear results are complementary with the surface roughness measurements of the coatings. Also, it can be observed that the wear of the C (nickel-based) coating is much lower.

Fig. 10 and 11 show the wear traces of M(Ni,Co)CrAlY coatings and Fig. 12 shows the wear trace of the Ni-based coating. All wear traces show the presence of oxides (primary oxides or material oxides due to wear). Also, it can be observed that the wear mechanism relies on smearing the coating material and, especially in the case of coating C, on low-cyclic fatigue resulting in the delamination of the coating material. The material removal is a result of cyclic compression and smearing of the HVOF-deposited material. Moreover, the observed delamination is in agreement with the splat dimensions indicating splat-induced detachment. Wear debris also plays a vital role due to its smearing through the wear trace and cyclic deformation leading to a fatigue detachment of the coating material.

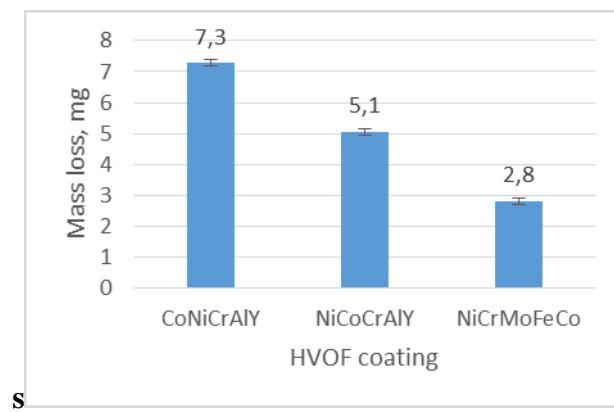


Fig. 6. Sliding wear results

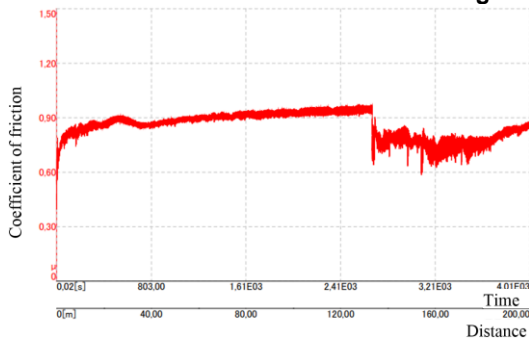


Fig. 7. Coefficient of friction vs. sliding distance, coating A (CoNiCrAlY)

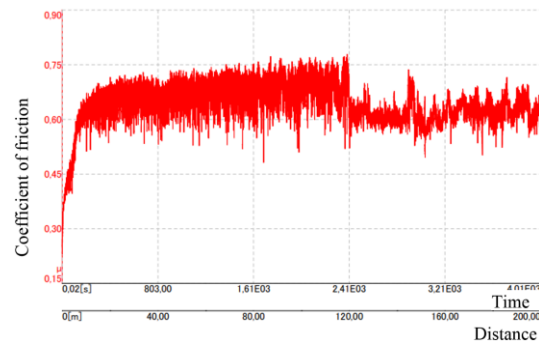


Fig. 8. Coefficient of friction vs. sliding distance, coating B (NiCoCrAlY)

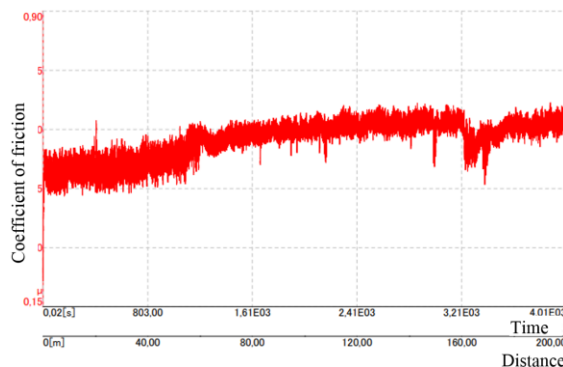
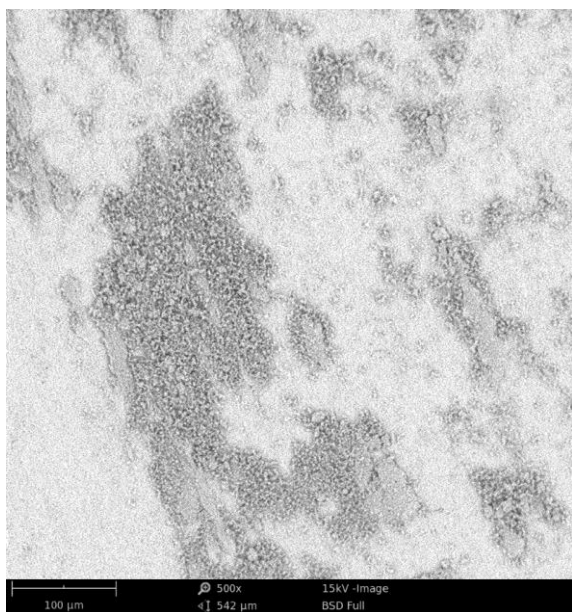
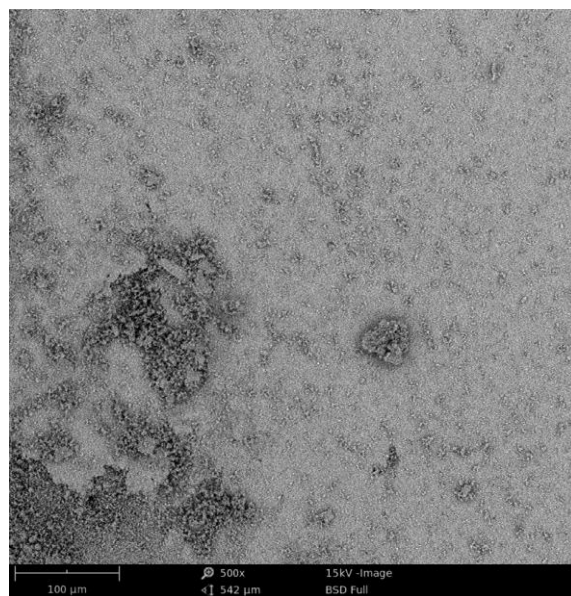
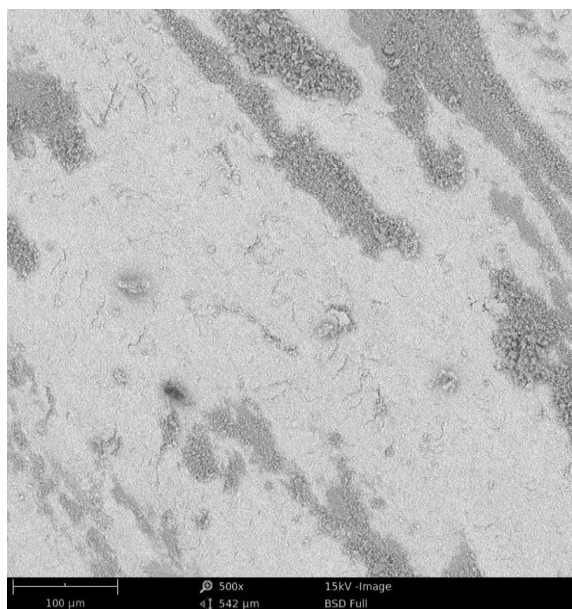


Fig. 9. Coefficient of friction vs. sliding distance coating C (NiCrMoFeCo)

Table 3. Friction coefficients of the tested coatings

Coating	Friction coefficient			
	Average	Min	Max.	SD
A	0.873	0.394	0.973	0.073
B	0.645	0.229	0.779	0.055
C	0.573	0.214	0.688	0.048

**Fig. 10.** Wear trace of coating A (CoNiCrAlY), SEM**Fig. 11.** Wear trace of coating B (NiCoCrAlY), SEM**Fig. 12.** Wear trace of coating C (NiCrMoFeCo), SEM

Cavitation erosion

Cavitation erosion curves of the HVOF coatings are given in Fig. 13. It can be observed that in comparison to M(Ni,Co)CrAlY, the C (nickel-based) coating exhibits higher resistance

to cavitation. The material loss of the coatings A and B are comparable, and it is twice higher than that of coating C. The mass loss of each thermally sprayed coatings is higher than those reported for HVOF sprayed CaviTec and Stellite-6 materials [23], as well as overlay welded nickel- and cobalt-based deposits [18,19]. The wear mechanism in the M(Ni,Co)CrAlY-type coatings is similar, and it consists in the detachment of loose splats and cracking induced by non-uniformities (unmelted particles, oxides, and lamellae borders). Material erosion is followed by plastic deformation of the coating material, as discussed in the previous study [49]. Fig. 14-16 show the cavitation-eroded surfaces of the HVOF coatings A, B, and C, respectively. A comparison of the SEM images reveals the presence of splat edges plastic deformation. Moreover, it can be observed that in the case of coating B the material is removed in massive chunks, while the C coating exhibits a much compact morphology and lower surface roughness, which increases its wear resistance. In contrast to coating C, the coatings A and B have a Ni-Co-based matrix. It seems that the deformability of nickel leads to an increased cavitation erosion resistance of coating C.

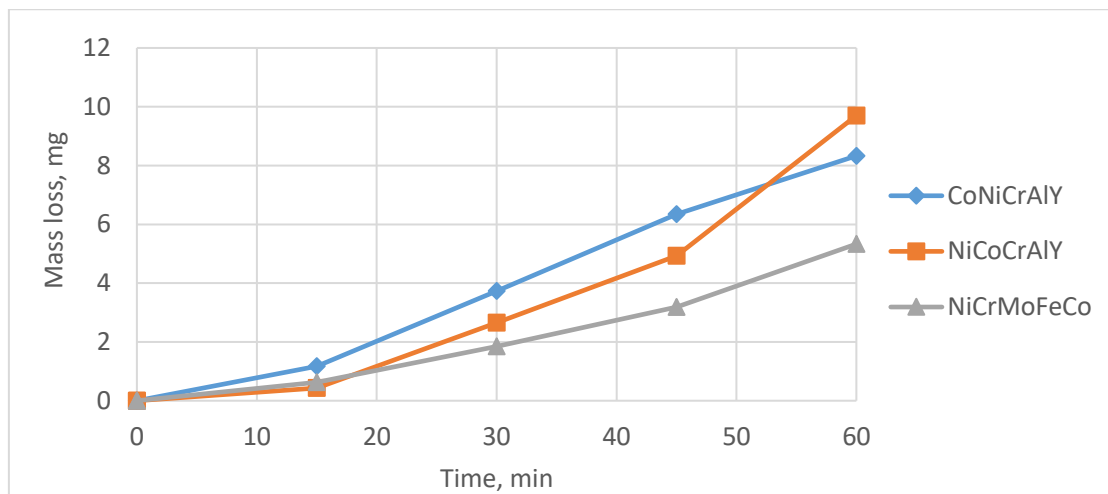


Fig. 13. Cavitation erosion curves of HVOF coatings

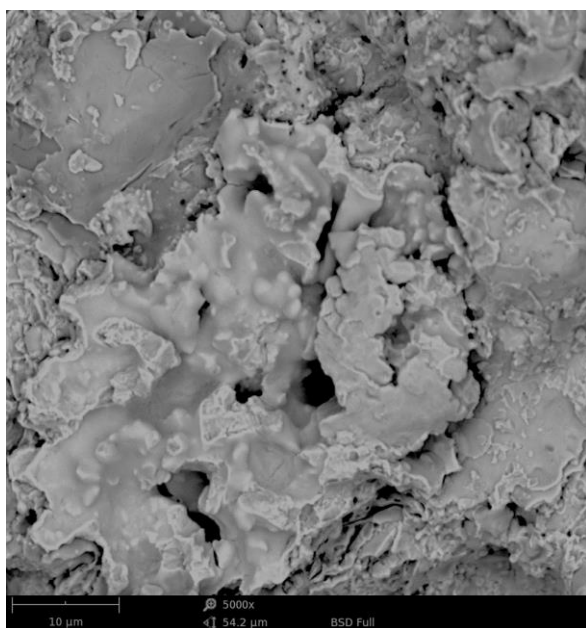


Fig. 14. Cavitation damaged surface of coating A (CoNiCrAlY), SEM

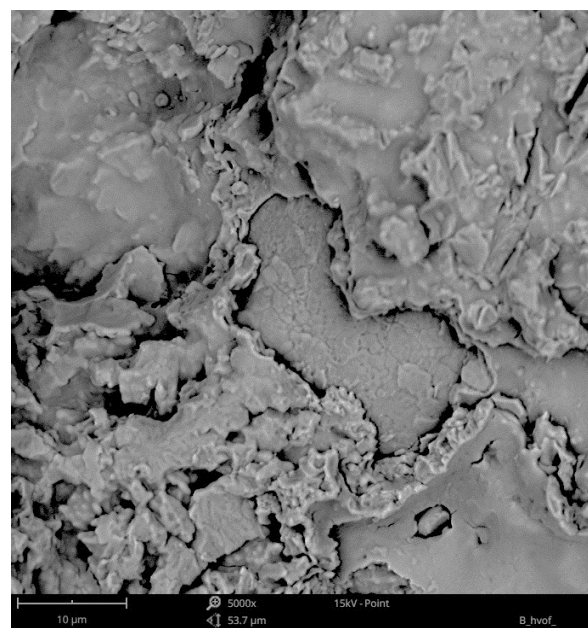


Fig. 15. Cavitation damaged surface of coating B (NiCoCrAlY), SEM

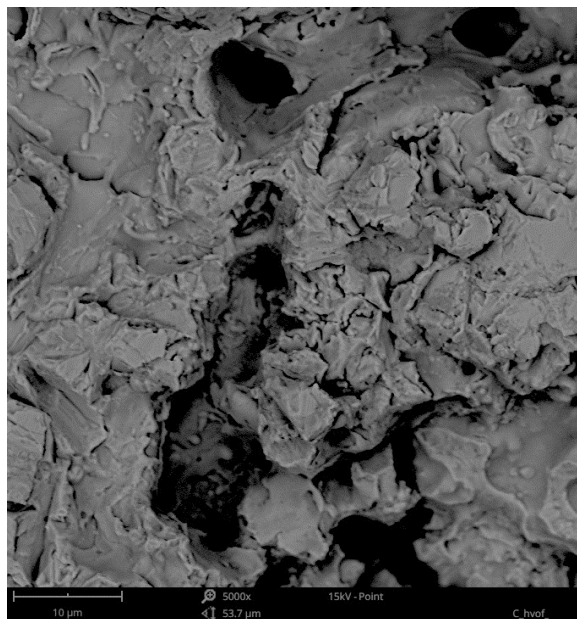


Fig. 16. Cavitation damaged surface of coating C (NiCrMoFeCo), SEM

CONCLUSIONS

The investigation into wear resistance is an up-to-date problem from the point of view of both scientific and engineering practice. In the present study, the sliding and cavitation erosion wear resistance of NiCrMoFeCo and MCrAlY (CoNiCrAlY and NiCoCrAlY) coatings was investigated. The coatings were deposited with means of the HVOF method. The results of the study lead to the following conclusions:

- the resistance to cavitation erosion of the M(Co,Ni)CrAlY coatings is almost two times lower than that of the NiCrMoFeCo deposit;
- the sliding wear resistance increases with increasing the nickel content as follows: CoNiCrAlY < NiCoCrAlY < NiCrMoFeCo;
- the friction coefficient increases with increasing the cobalt content as follows: NiCrMoFeCo < NiCoCrAlY < CoNiCrAlY;
- a combination of adhesive, oxidation and low-cyclic fatigue is the dominant sliding wear mechanism;
- cavitation erosion damage is induced by plastic deformation of the coating material; it is initiated at the non-uniform areas (unmelted particles, oxides, and lamellae borders) and results in the removal of the HVOF deposited material.

ACKNOWLEDGEMENTS

The project/research was financed in the framework of the project Lublin University of Technology - Regional Excellence Initiative, funded by the Polish Ministry of Science and Higher Education (contract no. 030/RID/2018/19).

REFERENCES

1. Krella, A.K.; Zakrzewska, D.E. Cavitation Erosion – Phenomenon and Test Rigs. *Adv. Mater. Sci.* 2018, 18, 15–26, doi:10.1515/adms-2017-0028.
2. Brennen, C.E. *Cavitation and Bubble Dynamics*; Oxford University Press: Oxford, 1995; ISBN 0-19-509409-3.
3. Soyama, H. Cavitation Peening: A Review. *Metals* 2020, 10, 270, doi:10.3390/met10020270.
4. Dular, M.; Osterman, A. Pit clustering in cavitation erosion. *Wear* 2008, 265, 811–820, doi:10.1016/j.wear.2008.01.005.
5. Franc, J.-P.; Michel, J.-M. *Fundamentals of Cavitation; Fluid Mechanics and Its Applications*; Kluwer Academic Publishers: New York, Boston, Dordrecht, London, Moscow, 2004; Vol. 76; ISBN 90-481-6618-7.
6. Gottardi, G.; Tocci, M.; Montesano, L.; Pola, A. Cavitation erosion behaviour of an innovative aluminium alloy for Hybrid Aluminium Forging. *Wear* 2018, 394–395, 1–10, doi:10.1016/j.wear.2017.10.009.
7. Szala, M. Application of computer image analysis software for determining incubation period of cavitation erosion – preliminary results. *ITM Web Conf.* 2017, 15, 06003, doi:10.1051/itmconf/20171506003.
8. Zakrzewska, D.E.; Krella, A.K. Cavitation Erosion Resistance Influence of Material Properties. *Adv. Mater. Sci.* 2019, 19, 18–34, doi:10.2478/adms-2019-0019.
9. Lin, J.; Wang, Z.; Cheng, J.; Kang, M.; Fu, X.; Hong, S. Effect of Initial Surface Roughness on Cavitation Erosion Resistance of Arc-Sprayed Fe-Based Amorphous/Nanocrystalline Coatings. *Coatings* 2017, 7, 200, doi:10.3390/coatings7110200.
10. Becker, W.T.; Shipley, R.J. *ASM Handbook, Volume 11: Failure Analysis and Prevention*; 10 edition.; ASM International: Materials Park, Ohio, 2002; ISBN 978-0-87170-704-8.
11. *ASM Handbook Volume 18: Friction, Lubrication, and Wear Technology*; ASM Handbook Volume 18.; ASM International, 1992; Vol. 18; ISBN 978-0-87170-380-4.
12. Szala, M.; Szafran, M.; Macek, W.; Marchenko, S.; Hejwowski, T. Abrasion Resistance of S235, S355, C45, AISI 304 and Hardox 500 Steels with Usage of Garnet, Corundum and Carborundum Abrasives. *Adv. Sci. Technol. Res. J.* 2019, 13, doi:10.12913/22998624/113244.
13. Jegadeeswaran, N.; Ramesh, M.R.; Bhat, K.U. Combating Corrosion Degradation of Turbine Materials Using HVOF Sprayed 25% (Cr₃C₂-25(Ni₂₀Cr)) + NiCrAlY Coating. *Int. J. Corros.* **2013**, 2013, 824659, doi:10.1155/2013/824659.
14. Szymański, K.; Hernas, A.; Moskal, G.; Myalska, H. Thermally sprayed coatings resistant to erosion and corrosion for power plant boilers - A review. *Surf. Coat. Technol.* 2015, 268, 153–164, doi:10.1016/j.surfcoat.2014.10.046.
15. Janicki, D. Microstructure and Sliding Wear Behaviour of In-Situ TiC-Reinforced Composite Surface Layers Fabricated on Ductile Cast Iron by Laser Alloying. *Materials* 2018, 11, 75, doi:10.3390/ma11010075.
16. Singh, J.; Kumar, S.; Mohapatra, S.K. An erosion and corrosion study on thermally sprayed WC-Co-Cr powder synergized with Mo₂C/Y₂O₃/ZrO₂ feedstock powders. *Wear* 2019, 438–439, doi:10.1016/j.wear.2019.01.082.
17. Singh, G.; Bala, N.; Chawla, V. Microstructural analysis and hot corrosion behavior of HVOF-sprayed Ni-22Cr-10Al-1Y and Ni-22Cr-10Al-1Y-SiC (N) coatings on ASTM-SA213-T22 steel. *Int. J. Miner. Metall. Mater.* 2020, 27, 401–416, doi:10.1007/s12613-019-1946-y.

18. Hattori, S.; Mikami, N. Cavitation erosion resistance of stellite alloy weld overlays. *Wear* 2009, 267, 1954–1960, doi:10.1016/j.wear.2009.05.007.
19. Szala, M.; Hejwowski, T.; Lenart, I. Cavitation erosion resistance of Ni-Co based coatings. *Adv. Sci. Technol. Res. J.* 2014, 8, 36–42, doi:10.12913/22998624.1091876.
20. Hejwowski, T. Sliding wear resistance of Fe-, Ni- and Co-based alloys for plasma deposition. *Vacuum* 2006, 80, 1326–1330, doi:10.1016/j.vacuum.2006.01.037.
21. Maslarevic, A.; Bakic, G.M.; Djukic, M.B.; Rajcic, B.; Maksimovic, V.; Pavkov, V. Microstructure and Wear Behavior of MMC Coatings Deposited by Plasma Transferred Arc Welding and Thermal Flame Spraying Processes. *Trans. Indian Inst. Met.* 2020, 73, 259–271, doi:10.1007/s12666-019-01831-9.
22. Janicki, D.M. High Power Diode Laser Cladding of Wear Resistant Metal Matrix Composite Coatings. *Solid State Phenom.* 2013, 199, 587–592, doi:10.4028/www.scientific.net/SSP.199.587.
23. Lavigne, S.; Pougoum, F.; Savoie, S.; Martinu, L.; Klemberg-Sapieha, J.E.; Schulz, R. Cavitation erosion behavior of HVOF CaviTec coatings. *Wear* 2017, 386–387, 90–98, doi:10.1016/j.wear.2017.06.003.
24. Zhang, P.; Jiang, J.H.; Ma, A.B.; Wang, Z.H.; Wu, Y.P.; Lin, P.H. Cavitation Erosion Resistance of WC-Cr-Co and Cr₃C₂-NiCr Coatings Prepared by HVOF. *Adv. Mater. Res.* 2007, 15–17, 199–204, doi:10.4028/www.scientific.net/AMR.15-17.199.
25. Szala, M.; Hejwowski, T. Cavitation Erosion Resistance and Wear Mechanism Model of Flame-Sprayed Al₂O₃-40%TiO₂/NiMoAl Cermet Coatings. *Coatings* 2018, 8, 254, doi:10.3390/coatings8070254.
26. Taillon, G.; Pougoum, F.; Lavigne, S.; Ton-That, L.; Schulz, R.; Bousser, E.; Savoie, S.; Martinu, L.; Klemberg-Sapieha, J.-E. Cavitation erosion mechanisms in stainless steels and in composite metal–ceramic HVOF coatings. *Wear* 2016, 364–365, 201–210, doi:10.1016/j.wear.2016.07.015.
27. Deng, W.; An, Y.; Hou, G.; Li, S.; Zhou, H.; Chen, J. Effect of substrate preheating treatment on the microstructure and ultrasonic cavitation erosion behavior of plasma-sprayed YSZ coatings. *Ultrason. Sonochem.* 2018, 46, 1–9, doi:10.1016/j.ultsonch.2018.04.004.
28. Szala, M.; Dudek, A.; Maruszczyk, A.; Walczak, M.; Chmiel, J.; Kowal, M. Effect of atmospheric plasma sprayed TiO₂-10% NiAl cermet coating thickness on cavitation erosion, sliding and abrasive wear resistance. *Acta Phys. Pol. A* 2019, 136, 335–341, doi:10.12693/APhysPolA.136.335.
29. Sugiyama, K.; Nakahama, S.; Hattori, S.; Nakano, K. Slurry wear and cavitation erosion of thermal-sprayed cermets. *Wear* 2005, 258, 768–775, doi:10.1016/j.wear.2004.09.006.
30. Łatka, L.; Szala, M.; Michalak, M.; Pałka, T. Impact of atmospheric plasma spray parameters on cavitation erosion resistance of Al₂O₃-13%TiO₂ coatings. *Acta Phys. Pol. A* 2019, 136, 342–347, doi:10.12693/APhysPolA.136.342.
31. Zhou, W.; Zhou, K.; Li, Y.; Deng, C.; Zeng, K. High temperature wear performance of HVOF-sprayed Cr₃C₂-WC-NiCoCrMo and Cr₃C₂-NiCr hardmetal coatings. *Appl. Surf. Sci.* 2017, 416, 33–44, doi:10.1016/j.apsusc.2017.04.132.
32. Saeidi, S.; Voisey, K.T.; McCartney, D.G. Mechanical Properties and Microstructure of VPS and HVOF CoNiCrAlY Coatings. *J. Therm. Spray Technol.* 2011, 20, 1231–1243, doi:10.1007/s11666-011-9666-5.
33. Singh, J.; Kumar, S.; Mohapatra, S.K. Tribological performance of Yttrium (III) and Zirconium (IV) ceramics reinforced WC–10Co₄Cr cermet powder HVOF thermally sprayed on X2CrNiMo-17-12-2 steel. *Ceram. Int.* 2019, 45, 23126–23142, doi:10.1016/j.ceramint.2019.08.007.

34. Hong, S.; Wu, Y.; Wang, Q.; Ying, G.; Li, G.; Gao, W.; Wang, B.; Guo, W. Microstructure and cavitation–silt erosion behavior of high-velocity oxygen–fuel (HVOF) sprayed Cr₃C₂–NiCr coating. *Surf. Coat. Technol.* 2013, 225, 85–91, doi:10.1016/j.surfcoat.2013.03.020.
35. Oksa, M.; Turunen, E.; Suhonen, T.; Varis, T.; Hannula, S.-P.; Oksa, M.; Turunen, E.; Suhonen, T.; Varis, T.; Hannula, S.-P. Optimization and Characterization of High Velocity Oxy-fuel Sprayed Coatings: Techniques, Materials, and Applications. *Coatings* 2011, 1, 17–52, doi:10.3390/coatings1010017.
36. Michalak, M.; Łatka, L.; Sokołowski, P.; Niemiec, A.; Ambroziak, A. The Microstructure and Selected Mechanical Properties of Al₂O₃ + 13 wt % TiO₂ Plasma Sprayed Coatings. *Coatings* 2020, 10, 173, doi:10.3390/coatings10020173.
37. Żórawski, W.; Kozerski, S. Scuffing resistance of plasma and HVOF sprayed WC₁₂Co and Cr₃C₂-25(Ni₂₀Cr) coatings. *Surf. Coat. Technol.* 2008, 202, 4453–4457, doi:10.1016/j.surfcoat.2008.04.045.
38. Ozimina, D.; Madej, M.; Kałdoński, T. The Wear Resistance of HVOF Sprayed Composite Coatings. *Tribol. Lett.* 2011, 41, 103–111, doi:10.1007/s11249-010-9684-3.
39. Benegra, M.; Santana, A.L.B.; Maranhão, O.; Pintaude, G. Effect of Heat Treatment on Wear Resistance of Nickel Aluminide Coatings Deposited by HVOF and PTA. *J. Therm. Spray Technol.* 2015, 24, 1111–1116, doi:10.1007/s11666-015-0266-7.
40. Potthoff, A.; Kratzsch, R.; Barbosa, M.; Kulissa, N.; Kunze, O.; Toma, F.-L. Development and Application of Binary Suspensions in the Ternary System Cr₂O₃-TiO₂-Al₂O₃ for S-HVOF Spraying. *J. Therm. Spray Technol.* 2018, 27, 710–717, doi:10.1007/s11666-018-0709-z.
41. Blum, M.; Krieg, P.; Killinger, A.; Gadow, R.; Luth, J.; Trenkle, F. High Velocity Suspension Flame Spraying (HVSFS) of Metal Suspensions. *Materials* 2020, 13, 621, doi:10.3390/ma13030621.
42. Tejero-Martin, D.; Pala, Z.; Rushworth, S.; Hussain, T. Splat formation and microstructure of solution precursor thermal sprayed Nb-doped titanium oxide coatings. *Ceram. Int.* 2020, 46, 5098–5108, doi:10.1016/j.ceramint.2019.10.253.
43. Kiilakoski, J.; Musalek, R.; Lukac, F.; Koivuluoto, H.; Vuoristo, P. Evaluating the toughness of APS and HVOF-sprayed Al₂O₃-ZrO₂-coatings by in-situ- and macroscopic bending. *J. Eur. Ceram. Soc.* 2018, 38, 1908–1918, doi:10.1016/j.jeurceramsoc.2017.11.056.
44. Pawłowski, L. 5 - Application of solution precursor spray techniques to obtain ceramic films and coatings. In *Future Development of Thermal Spray Coatings*; Espallargas, N., Ed.; Woodhead Publishing, 2015; pp. 123–141 ISBN 978-0-85709-769-9.
45. Myalska, H.; Lusvarghi, L.; Bolelli, G.; Sassatelli, P.; Moskal, G. Tribological behavior of WC-Co HVAF-sprayed composite coatings modified by nano-sized TiC addition. *Surf. Coat. Technol.* 2019, 371, 401–416, doi:10.1016/j.surfcoat.2018.09.017.
46. Vijay, S.; Wang, L.; Lyphout, C.; Nylen, P.; Markocsan, N. Surface characteristics investigation of HVAF sprayed cermet coatings. *Appl. Surf. Sci.* 2019, 493, 956–962, doi:10.1016/j.apsusc.2019.07.079.
47. Nowak, W.J.; Ochał, K.; Wierzba, P.; Gancarczyk, K.; Wierzba, B. Effect of Substrate Roughness on Oxidation Resistance of an Aluminized Ni-Base Superalloy. *Metals* 2019, 9, 782, doi:10.3390/met9070782.
48. Szala, M.; Beer-Lech, K.; Gancarczyk, K.; Kilic, O.B.; Pędrak, P.; Özer, A.; Skic, A. Microstructural Characterisation of Co-Cr-Mo Casting Dental Alloys. *Adv. Sci. Technol. Res. J.* 2017, 11, 76–82, doi:10.12913/22998624/80901.

49. Szala, M.; Walczak, M. Cavitation erosion and sliding wear resistance of HVOF coatings. *Weld. Technol. Rev.* 2018, 90, doi:10.26628/wtr.v90i10.964.
50. ASTM G32-10: Standard Test Method for Cavitation Erosion Using Vibratory Apparatus; ASTM International: West Conshohocken, Philadelphia: PA, USA, 2010;
51. Szala, M.; Walczak, M.; Pasierbiewicz, K.; Kamiński, M. Cavitation Erosion and Sliding Wear Mechanisms of AlTiN and TiAlN Films Deposited on Stainless Steel Substrate. *Coatings* 2019, 9, 340, doi:10.3390/coatings9050340.
52. Davis, J.R. *Handbook of Thermal Spray Technology*; ASM International: OH, USA, 2004; ISBN 978-0-87170-795-6.
53. Maruszczuk, A.; Dudek, A.; Szala, M. Research into Morphology and Properties of TiO₂ – NiAl Atmospheric Plasma Sprayed Coating. *Adv. Sci. Technol. Res. J.* 2017, 11, 204–210, doi:10.12913/22998624/76450.
54. Cabral-Miramontes, J.A.; Gaona-Tiburcio, C.; Almeraya-Calderón, F.; Estupiñan-Lopez, F.H.; Pedraza-Basulto, G.K.; Poblano-Salas, C.A. Parameter Studies on High-Velocity Oxy-Fuel Spraying of CoNiCrAlY Coatings Used in the Aeronautical Industry. *Int. J. Corros.* 2014, 2014, 703806, doi:10.1155/2014/703806.
55. Walczak, M.; Pieniak, D.; Niewczas, A.M. Effect of recasting on the useful properties CoCrMoW alloy. *Eksplloat. Niezawodn. – Maint. Reliab.* 2014, 16, 330–336.